Published in final edited form as:
Mol Microbiol. 2006 May ; 60(4): 1026–1043. doi:10.1111/j.1365-2958.2006.05156.x.

Analysis of FimX, a phosphodiesterase that governs twitching motility in *Pseudomonas aeruginosa*

Barbara I. Kazmierczak[1,2,*], **Maria B. Lebron**[1,2], and **Thomas S. Murray**[1,2,3]

[1]Department of Internal Medicine, Yale University School of Medicine, 333 Cedar St., New Haven, CT 06520-8022, USA

[2]Department of Microbial Pathogenesis, Yale University School of Medicine, 333 Cedar St., New Haven, CT 06520-8022, USA

[3]Department of Pediatrics, Yale University School of Medicine, 333 Cedar St., New Haven, CT 06520-8022, USA

Summary

Type IV pili (Tfp) are polar surface structures of *Pseudomonas aeruginosa* required for twitching motility, biofilm formation and adherence. One protein required for the assembly of tfp is FimX, which possesses both GGDEF and EAL domains characteristic of diguanylate cyclases and phosphodiesterases respectively. In this work we demonstrate that FimX has phosphodiesterase activity towards bis-(3′-5′)-cyclic dimeric guanosine monophosphate (c-di-GMP), but does not show diguanylate cyclase activity. Instead, the imperfect GGDEF domain of FimX likely serves to activate phosphodiesterase activity when bound to GTP, as has recently been described for the *Caulobacter crescentus* composite GGDEF-EAL protein, CC3396. Bacteria expressing FimX in which either the GGDEF or EAL domain is deleted or mutated have phenotypes indistinguishable from a Δ*fimX* strain, demonstrating the importance of both domains to function. Previous work has shown that FimX localizes to the bacterial pole. In this work we show that restriction of FimX to a single pole requires intact GGDEF and EAL domains. Deletion of the amino-terminal REC domain of FimX, which contains a putative polar localization signal, results in a protein that still supports intermediate levels of pilus assembly and function. RFP–FimXΔREC, unlike RFP–FimX, is no longer localized to the bacterial pole, while transmission electron microscopy shows that surface pili can originate from non-polar sites in this mutant. Although Δ*fimX* mutants show limited *in vitro* cytotoxicity, they are as virulent as the wild-type strain in a murine model of acute pneumonia.

Introduction

The Gram-negative bacterium *Pseudomonas aeruginosa* is a ubiquitous environmental organism which causes a variety of opportunistic infections in human hosts. These include severe acute infections in individuals with local or systemic compromise of host defences, such as burn patients, persons on mechanical ventilators, or patients receiving chemotherapy. *P. aeruginosa* also causes chronic infections associated with significant morbidity and mortality in patients with cystic fibrosis. *P. aeruginosa* can infect a broad spectrum of model organisms, including plants, nematodes, insects and mice, and employs a large set of virulence factors to enable colonization, persistence and dissemination in these varied sites. These include surface organelles, namely type IV pili (tfp) and flagella, which

*For correspondence. barbara.kazmierczak@yale.edu; Tel. (+1) 203 737 5062; Fax (+1) 203 785 3864.

play important roles in motility, adhesion and biofilm formation; secreted degradative enzymes and toxins, which lead to tissue damage and cell death; and translocated substrates of the type III secretion system (TTSS), which disrupt host signal transduction pathways and cause cytotoxicity and necrosis (Salyers and Whitt, 2002). The expression of these virulence factors is regulated in response to incompletely understood environmental cues. The proteins which sense and respond to such environmental stimuli are of great interest, both as keys to understanding basic pathogenic mechanisms of Pseudomonas and as targets for therapies that might disrupt pathogenesis.

Type IV pili are thin, flexible filaments localized to the poles of *P. aeruginosa* (recently reviewed in Mattick, 2002). Through a cycle of extension, attachment and retraction, tfp mediate bacterial movement over solid surfaces in a process called twitching motility (Bradley, 1980; Merz *et al.*, 2000). Tfp also serve as receptors for bacteriophages (Bradley, 1980), facilitate bacterial attachment to eukaryotic cell surfaces (Woods *et al.*, 1980; Doig *et al.*, 1988; Chi *et al.*, 1991; Comolli *et al.*, 1999a), and contribute to biofilm formation (O'Toole and Kolter, 1998; Klausen *et al.*, 2003a,b). Tfp are polymers composed of pilin, the product of the *pilA* gene (Sastry *et al.*, 1985). The assembly of functional pili on the bacterial surface requires approximately 40 gene products (Mattick, 2002). Many of these proteins are required for assembly (extension) and retraction of the pilus; however, another group of proteins appears to play regulatory roles, controlling either the expression of proteins required for tfp assembly or regulating tfp-dependent motility in response to environmental cues. Tfp expression appears to be co-ordinately regulated with that of other virulence factors primarily via Vfr, a cAMP-binding protein which affects not only tfp and flagellar biosynthesis, but also the expression of Type II general secretory pathway substrates, TTSS substrates and apparatus, and quorum sensing. Other regulatory proteins involved in tfp assembly include the sensor kinase/response regulator pairs PilS/PilR and FimS/AlgR, the complex multidomain regulator ChpA (Whitchurch *et al.*, 2004), and FimL, a recently described regulator which may function by controlling *vfr* expression (Whitchurch *et al.*, 2005).

In this work we focus on FimX, a protein which appears to have a regulatory role in surface assembly of pili (Huang *et al.*, 2003). As noted by Huang *et al.*, FimX possesses GGDEF (aa 260–424, *E*-value $3.8e^{-12}$) and EAL (aa 439–683, *E*-value $3.4e^{-41}$) domains (http://pfam.wustl.edu), which are found in more than 2000 Gram-positive and Gram-negative bacterial proteins (Romling *et al.*, 2005). A significant number of GGDEF and EAL domain proteins described to date appear to play roles in the co-ordinate regulation of motility, adherence, and complex multicellular phenotypes such as biofilm formation, colony morphology and autolysis. GGDEF and EAL domain proteins also appear to be relevant to host-pathogen interactions. A number of proteins with GGDEF domains have now been shown act as diguanylate cyclases (DGCs), carrying out the synthesis of bis-(3′-5′)-cyclic dimeric guanosine monophosphate (c-di-GMP) from two molecules of GTP (Paul *et al.*, 2004). The EAL domain has recently been shown to be sufficient for the hydrolysis of c-di-GMP into linear dimeric GMP, pGpG, and thus possesses phosphodiesterase-A (PDE-A) activity (Schmidt *et al.*, 2005). Although many proteins possess both GGDEF and EAL domains, all such dual domain proteins tested for enzymatic activity *in vitro* appear to show only one activity; however, there are *in vivo* observations which suggest that GGDEF-EAL domain proteins may exhibit both (Romling *et al.*, 2005). The amino-terminus of FimX contains REC (*E*-value 0.0018) and PAS domains (*E*-value $4.9e^{-6}$). REC, or CheY domains, are commonly found in response regulators of two component phosphorelays, and characteristically have an aspartate residue that serves as a phosphoryl acceptor (Hoch and Silhavy, 1995). The REC domain of FimX (aa 8–127) lacks a candidate catalytic aspartate, suggesting that this domain is unlikely to be activated by phosphorylation; however, a possible polar localization domain, as mapped by Huang *et al.* (2003), resides at the end of

the REC domain. PAS domains (aa 144–208) are commonly found in signalling proteins and appear to allow oxygen and redox potential to be sensed (Zhulin and Taylor, 1997).

We have constructed and analysed a series of domain deletion and point mutants of FimX. We report here that both GGDEF and EAL domains of FimX appear to contribute to its biological function in *P. aeruginosa*. Purified FimX exhibits *in vitro* phosphodiesterase activity which is strongly stimulated in the presence of GTP, but lacks detectable DGC activity. Mutation of the EAL domain abolishes phosphodiesterase activity; mutation of the GGDEF domain does likewise. Lastly, we present data demonstrating that intact GGDEF and EAL domains are required for the observed localization of FimX to a single bacterial pole.

Results

ΔfimX bacteria have defects in assembly of tfp and in twitching motility

We initially discovered FimX (PA4959) as the site of a transposon insertion that rendered PA103*pscJ*::SMIT, an invasive, TTSS^{-} strain, no longer invasive for epithelial cells (B.I. Kazmierczak, M.B. Lebron, C. Nelson, R. Kowal, M. Ledizet, J.N. Engel, unpubl. data). We subsequently constructed an unmarked deletion of aa 15–685 of FimX in PA103, a well-characterized clinical isolate of *P. aeruginosa* that is highly cytotoxic towards cultured epithelial cells. PA103 expresses tfp, surface appendages required for twitching motility, sensitivity to the pilus-specific phage PO4 and biofilm formation (Bradley, 1980; O'Toole and Kolter, 1998). We found that Δ*fimX* bacteria showed diminished twitching motility as measured by sub-surface stab assays (Table 1), altered colony morphology (Fig. 1) and decreased phage sensitivity (Table 1). These defects were fully complemented by expression of FimX, either from a high-copy number plasmid or from a single copy of the gene integrated at the chromosomal *attB* site. Our findings corroborate those of Huang *et al.* who independently discovered FimX in a screen for mutants of PAK that had lost the ability to twitch and published their findings while this work was in progress (Huang *et al.*, 2003). The loss of twitching motility in Δ*fimX* is due to a failure to assemble surface pili; the pilin subunit, PilA, is still produced in this mutant (Huang *et al.*, 2003).

We also constructed an epitope-tagged version of FimX, BB2–FimX, in which the BB2 epitope tag (EVHTNQDPLD) (Brookman *et al.*, 1995) was introduced after the initiating methionine of FimX by PCR. We confirmed that BB2–FimX complemented a Δ*fimX* mutant fully for phage sensitivity and twitching motility (data not shown). We also constructed BB2 epitope-tagged versions of all mutant alleles of FimX which we subsequently designed, allowing us to determine protein levels for these mutant constructs.

Construction and expression of domain deletion mutants of FimX

FimX possesses REC (response regulator), PAS, GGDEF and EAL domains, as defined in the Pfam 17.0 (March 2005) database (http://pfam.wustl.edu). In order to test whether these domains are required for FimX function, we constructed a series of deletion mutants lacking aa 67–147 (ΔREC), aa 253–443 (ΔGGDEF) or aa 445–691 (ΔEAL) (Fig. 2A). These mutations were introduced into native FimX and into the BB2 epitope-tagged FimX construct. All constructs were expressed from a high-copy number plasmid (under control of the native promoter) and as a single gene copy integrated into the chromosome at the *attB* site, also under control of the *fimX* promoter. As seen in Fig. 2B, all of the domain deletion constructs appear to be stably expressed in PA103 at comparable steady-state levels.

Both GGDEF and EAL domains are required for twitching motility and phage sensitivity

The Δ*fimX* mutant fails to assemble functional pili. We assayed whether the ΔREC, ΔGGDEF or ΔEAL derivatives of FimX could assemble functional pili. As seen in Table 1 and Fig. 1, the ΔREC mutant appears to restore partial pilus function, as assayed by sensitivity to phage PO4 and by colony morphology. We can also detect surface pili on Δ*fimX* bacteria expressing FimXΔREC (Fig. 3); however, organized movement of bacteria, as assayed by twitching motility zone size, is not fully complemented. Δ*fimX* bacteria expressing FimXΔGGDEF have similar levels of surface pilin expression and phage sensitivity as the uncomplemented mutant. Expression of the FimXΔEAL allele reproducibly resulted in decreased levels of surface pili and phage sensitivity as compared with the Δ*fimX* strain.

Point mutations in the GGDEF and EAL motifs recapitulate ΔGGDEF and ΔEAL phenotypes

The protein crystal structure of a diguanylate cyclase, PleD, has recently been published (Chan *et al.*, 2004). This structure demonstrates the importance of residues within the GGDEF motif for contacts crucial to substrate binding and catalysis. The corresponding amino acids in FimX are GDSIF, which raises the question of whether this protein is a true DGC. Using site-directed mutagenesis, we substituted alanines for both Gly346 and Asp347 (GDSIF→AASIF) to test the importance of this motif for FimX function. The sequence of FimX at the proposed PDE active site is EVL, which is a variant of EAL found in proteins with documented PDE activity (Schmidt *et al.*, 2005). However, a recent analysis by Gomelsky and colleagues attempted to identify additional sequences within EAL domains which would distinguish whether the proteins were likely to show phosphodiesterase activity (Schmidt *et al.*, 2005). Many of these conserved residues are not present in FimX, raising the question of whether the protein is likely to have an active EAL domain. We therefore mutated the amino acids Glu475, Val476 and Leu477 to alanines (EVL→AAA) to test whether the phosphodiesterase domain of the protein contributes to its activity. Both mutations were introduced into Δ*fimX* bacteria as native and BB2-tagged proteins expressed under the *fimX* promoter on a high-copy number plasmid. Steady-state protein levels of both FimX(GDSIF→AASIF) and FimX(EVL→AAA) were comparable with those of wild-type protein (Fig. 4A). However, the phenotypes of bacteria expressing these mutant alleles of FimX were indistinguishable from the null mutant. Neither FimX(GDSIF→AASIF) nor FimX(EVL→AAA) restored twitching activity or PO4 phage sensitivity to Δ*fimX* bacteria (Table 1). Determination of surface pili by enzyme-linked immunosorbent assay (ELISA) showed that bacteria expressing either point mutant allele of FimX failed to assemble surface pili (Fig. 4B). Thus the GGDEF and EAL domains appear to be critical for FimX function *in vivo*, and both the EVL and non-canonical GDSIF motifs are functionally essential.

FimX exhibits phosphodiesterase, but not DGC, activity *in vitro*

Wild-type FimX, FimX(GDSIF→AASIF) and FimX(EVL→AAA) were expressed as His_6 fusion proteins in *Escherichia coli*, purified by affinity chromatography and assayed to determine whether these proteins possess detectable DGC and/or phosphodiesterase activity. As shown in Fig. 5A, neither wild-type nor mutant alleles of His_6-FimX could catalyse c-di-GMP formation. We were readily able to detect DGC activity of the *Caulobacter crescentus* proteins PleD-His_6 and PleD*-His_6; mutations in the latter allele render it about 100-fold more active a DGC than wild-type PleD (Paul *et al.*, 2004). FimX activity was assayed in the presence of several divalent cations in addition to Mg^{2+}, including Mn^{2+}, Zn^{2+} and Ca^{2+}, and in the presence of the reducing agent dithiotreitol (1 μM−10 mM) (data not shown); however, we did not detect c-di-GMP production under any of these conditions.

We used PleD* to synthesize [^{32}P]-c-di-GMP from [^{32}P]-GTP; this was then used as the substrate for phosphodi-esterase assays. As shown in Fig. 5B, *C. crescentus* CC3396, which served as a positive control, catalysed hydrolysis of c-di-GMP into pGpG. As previously described, the reaction was activated by the addition of 100 μM GTP (Christen *et al.*, 2005). FimX was also able to convert c-di-GMP into pGpG and, like CC3396, its PDE activity was significantly increased by the presence of GTP in the reaction mix. His_6-FimX(GDSIF→AASIF) and His_6-FimX(EVL→AAA) were also assayed under these conditions. As seen in Fig. 5C, neither mutant protein produced pGpG when assayed in the presence of 10 mM $MgCl_2$, regardless of the presence or absence of GTP. This suggests that FimX may be similar to CC3396, a phosphodiesterase in which a degenerate GGDEF domain (GEDEF) binds GTP and allosterically activates PDE activity resident within the EAL domain (Christen *et al.*, 2005). As observed for CC3396, neither FimX nor the point mutant alleles show PDE-A activity when assayed in the presence of Ca^{2+}, despite the addition of 100 μM GTP (Fig. 5C).

Bobrov and colleagues recently described an assay that utilizes bis(*p*-nitrophenyl) phosphate as a surrogate substrate for EAL domain proteins (Bobrov *et al.*, 2005). Using this assay, they found that the EAL domain of *Yersinia pestis* HmsP produced *p*-nitrophenol in the presence of Mn^{2+}, but not when the divalent cation Mg^{2+} was used instead. We also examined the effect of Mn^{2+} on PDE activity of FimX and CC3396, using the substrate c-di-GMP (Fig. 5C). For both CC3396 and FimX, Mn^{2+} appeared to increase PDE activity, both in the presence and absence of GTP. Interestingly, the FimX point mutants showed a different pattern of response to Mn^{2+}: both showed some pGpG production in the absence of GTP, but were no longer activated by the addition of GTP. As a control, we incubated c-di-GMP with 10 mM $MnCl_2$ in the absence of protein for 60 min and did not detect hydrolysis. Furthermore, the effect of adding $MnCl_2$ varied with each protein assayed. These findings suggested that Mn^{2+} was likely affecting the interaction of the various PDEs with substrate. Mn^{2+}, however, was neither sufficient to catalyse c-di-GMP breakdown itself, nor acting through a common component present in the reactions (i.e. a co-purified *E. coli* protein or PleD* that had survived the 10 min 95°C incubation step of c-di-GMP preparation).

Localization of FimX to the pole requires two signals

Huang *et al.* (2003) had demonstrated that a RFP–FimX fusion could be localized a single bacterial pole, and that a truncated fusion protein containing only the amino terminal 154 aa of FimX was correctly localized to the pole. Although no clear consensus sequence for polar localization has been defined, Huang *et al.* attempted to align the terminal 35 aa of the truncated FimX sequence with amino acid sequences implicated in polar localization of proteins in other bacteria. All of the amino acid residues that they identify as potential determinants of a polar localization signal in FimX are absent in our ΔREC allele, raising the question of whether ΔREC is appropriately localized to the bacterial pole. We addressed this by constructing RFP fusion proteins to FimX and FimXΔREC, which we expressed in Δ*fimX* bacteria from the pUCP-SK plasmid under control of the *fimX* promoter. (We could not detect any of the fusion proteins when they were expressed from a single copy of the gene integrated into the chromosomal *attB* site.) The RFP–FimX fusion restored twitching motility to Δ*fimX* bacteria, demonstrating that the fusion protein retained function (data not shown). As seen in Fig. 6A, RFP–FimX localized predominantly to one bacterial pole, confirming the observations of Huang *et al.* Wild-type or Δ*fimX* bacteria expressing RFP alone showed no polar localization of fluorescence (Fig. 6B and data not shown). Most bacteria failed to localize the RFP–ΔREC fusion to the poles, suggesting that assembly of tfp that supported PO4 phage infection did not absolutely require polar localization of FimX. We also constructed RFP fusions to the two point mutant alleles of FimX to determine whether the putative DGC and PDE activities of FimX influenced localization. The RFP–

FimX(GDSIF→AASIF) and RFP–FimX(EVL→AAA) constructs showed predominantly bipolar localization in the Δ*fimX* background. Chi-square analysis confirmed that the distribution of RFP–FimX was significantly different from that of RFP–ΔREC ($\chi^2 = 147.3$, $P < 0.0001$), of RFP–FimX(GDSIF→AASIF) ($\chi^2 = 75.5$, $P < 0.0001$) and of RFP–FimX(EVL→AAA) ($\chi^2 = 57.56$, $P < 0.0001$). The two point mutants, however, showed similar patterns of distribution ($\chi^2 = 3.153$, $P = 0.21$). As neither point mutant is capable of complementing twitching motility, we hypothesized that the unipolar localization seen for the RFP–FimX might require bacterial motility, in which case the mutant fusion proteins would localize correctly when expressed in the PA103 background. Conversely, unipolar localization might require an enzymatically active FimX protein, in which case the mutant fusion proteins would remain bipolar in PA103. As seen in Fig. 6B, both mutant fusion proteins show a predominantly bipolar distribution in wild-type PA103. We again tallied the localization pattern of the RFP fusions for > 100 bacteria [RFP–FimX(GDSIF→AASIF): unipolar = 26 (23%), bipolar = 75 (66%), non-polar = 12 (11%); RFP–FimX(EVL→AAA): unipolar = 45 (28%), bipolar = 87 (55%), non-polar = 26 (16%)]. Thus expression of the point mutant proteins in a wild-type background is not sufficient to restrict their localization to a single pole. Of note, neither point mutant inhibits twitching motility of wild-type PA103, even when expressed from a high-copy number plasmid (data not shown).

Localization of tfp is altered in bacteria expressing FimXΔREC

Our observation that RFP–FimXΔREC fails to localize to the poles prompted us to examine whether pili have the same localization in FimXΔREC as in wild-type PA103. PA103 pUCP-SK and Δ*fimX* pΔREC bacteria were visualized by transmission electron microscopy (TEM) to examine pilus location. Only bacteria which were well-separated from other bacteria were examined, to minimize artifacts caused by a bacterium overlying tfp originating from other cells. As seen in Fig. 7, PA103 bacteria usually have pili that arise at or near the poles; no flagella are seen, as expected for this hypoflagellated, non-swimming strain. In contrast, Δ*fimX* pFimXΔREC bacteria had pili that originated from non-polar as well as polar sites on the bacterial surface, suggesting that correctly localized FimX may play a role in restricting pilus assembly to the bacterial poles.

FimX is required for in vitro cytotoxicity but not for in vivo virulence

The presence of functional pili is strongly correlated with the ability of bacteria to cause epithelial cell cytotoxicity *in vitro* (Kang *et al.*, 1997). Whether the pili serve as adhesins, or play a more active role in regulating the TTSS is an area of active debate (Sundin *et al.*, 2002). We tested whether Δ*fimX* bacteria had any defects in cytotoxicity. As seen in Fig. 8A, Δ*fimX* bacteria were less cytotoxic than PA103 when assayed at 2 hours post infection (hpi) (*c.* 33% of wild-type) and 4 hpi (*c.* 46% of wild-type). This defect could be complemented by transforming Δ*fimX* with a plasmid expressing FimX under control of its own promoter, or by expressing FimX from an ectopic copy of the gene integrated into the Δ*fimX* chromosome at the *attB* site (Δ*fimX attB::*FimX) (Fig. 8A and data not shown). Rapid cytotoxicity under these conditions is primarily due to ExoU, a phospholipase which is translocated into host cells by the TTSS (Finck-Barbancon *et al.*, 1997; Hauser *et al.*, 1998; Sato *et al.*, 2003). We therefore tested whether the TTSS was intact in Δ*fimX* by growing this mutant in MinS, which induces TTSS effector production and secretion *in vitro* (Frank, 1997). Δ*fimX* produced and secreted ExoU, ExoT, and the translocon components PopB, PopD and PcrV identically to wild-type PA103 under these conditions (data not shown). Thus, deletion of FimX does not appear to affect the function or regulation of the TTSS apparatus and effectors *in vitro*. Δ*fimX* growth curves in Luria–Bertani broth (LB) and minimal media [(MinS and Vogel–Bonner minimal (VBM)] were indistinguishable from those of wild-type PA103, arguing that a growth defect of the mutant could not account for the observed reduction in cytotoxicity (data not shown). Δ*fimX* bacteria were

deficient, however, in binding to epithelial cells, a phenotype also described for Δ*pilA* mutants of *P. aeruginosa* (Comolli *et al.*, 1999a; Sundin *et al.*, 2002). Thus, in binding assays measuring the percentage of a bacterial inoculum adherent to HeLa cells 1 hpi, we observed that the number of ΔUTΔ*fimX* bacteria bound was about 8% of the ΔUT control (range 2.1–16%, $n = 8$ independent experiments carried out in triplicate). This is comparable to the efficiency with which Δ*pilA* bacteria appear to bind HeLa cells, both in our hands (3–5% of isogenic wild-type control) and in published studies (2–4% of isogenic wild-type control as reported by Sundin *et al.*).

Next, we examined whether Δ*fimX* bacteria were able to cause disease in the murine acute pneumonia model. Eight- to 10-week-old C57Bl/6 female mice were infected with 5×10^5 PA103 or Δ*fimX* via the nares, then euthanized at 16 hpi. Both groups of mice appeared ill at this time point, as evidenced by hunched posture, laboured breathing and ruffled fur. Δ*fimX* bacteria were recovered from infected lungs and livers in numbers greater than those of wild-type PA103 (Fig. 8B). This strongly argues that Δ*fimX* bacteria are able to utilize the TTSS and its effectors during *in vivo* infection, because isogenic mutants which do not express positive regulators of TTSS, such as ExsA or RtsM/RetS, are effectively cleared from the lung in this time (Goodman *et al.*, 2004; Laskowski *et al.*, 2004). Of note, Δ*pilA P. aeruginosa* strains also retain virulence in murine models of acute infection (Comolli *et al.*, 1999b; Kulesekara *et al.*, 2006).

Discussion

Both GGDEF and EAL motifs appear to contribute to FimX function

FimX belongs to the large family of bacterial proteins which contain GGDEF and/or EAL domains. These domains have been shown to possess DGC and phosphodiesterase activity respectively. As such, proteins with DGC or PDE activity have the capacity to regulate the amount of c-di-GMP in the bacterial cell. Biochemical analyses of purified GGDEF and EAL domains have provided additional information regarding sequences important for enzymatic activity. Thus, the DGC PleD of *C. crescentus*, for which both biochemical (Paul *et al.*, 2004) and structural (Chan *et al.*, 2004) data exist, possesses an active site (A-site) which contains the GGEEF signature motif and which binds c-di-GMP in the PleD/c-di-GMP cocrystal. PleD contains an additional site at which a c-di-GMP dimer was found to bind; binding at this 'I-site' appears to inhibit DGC activity allosterically. Amino acid substitutions within the GGDEF motif are poorly tolerated. Thus substitution by alanine of any residue within the GGEEF motif of the *Y. pestis* HmsT protein results in a complete loss of *Y. pestis* biofilm formation equivalent to that seen in a $HmsT^-$ mutant (Kirillina *et al.*, 2004). Mutation of the GGEEF motif of PleD to DEEEF similarly results in the loss of PleD function vis-a-vis stalk biogenesis (Aldridge and Jenal, 1999) and abolishes *in vitro* DGC activity of PleD (Paul *et al.*, 2004). This would argue that an imperfect A-site motif, such as the GDSIF sequence present in FimX, is unlikely to catalyse c-di-GMP synthesis. Indeed, we cannot detect DGC activity of purified FimX *in vitro*.

FimX nonetheless does not tolerate amino acid changes at its imperfect A-site motif, as shown by the loss of function of the FimX(GDSIF→AASIF) allele. Christen *et al.* (2005) have recently reported that an imperfect A-site motif (GEDEF) in the *C. crescentus* protein CC3396 is still capable of binding GTP. This protein, which also has an EAL domain, has no demonstrable DGC activity *in vitro* but does possess phosphodiesterase activity. Interestingly, binding of GTP by CC3396 increases the phosphodiesterase activity of the protein some 40-fold; a mutant version of CC3396, in which the GEDEF motif is mutated to GQNEF, shows only threefold increase of PDE activity in response to GTP (Christen *et al.*, 2005). We have found that FimX also shows phosphodiesterase activity towards c-di-GMP, and that this activity is stimulated by the presence of 100 μM GTP. When the GDSIF motif

of FimX is mutated, GTP no longer stimulates PDE activity of FimX, suggesting that this imperfect A-site motif may be playing an analogous role to the GEDEF sequence of CC3396. The PDE-A activity of FimX, CC3396 and the two FimX point mutants also appears to be stimulated more effectively by Mn^{2+} than by Mg^{2+}. Similar effects of Mn versus Mg on catalytic activity have been described for mammalian phosphodiesterases that hydrolyse cAMP or cGMP (Francis *et al.*, 2000). The biological significance of this finding is not clear, however, as concentrations of Mg^{2+} are approximately two orders of magnitude greater than those of Mn^{2+} in bacterial cells (De Medicis *et al.*, 1986).

In a recent publication, Schmidt *et al.* (2005) compare a number of EAL domain containing proteins and define sequences beyond the EAL motif itself which are conserved among proteins that show phosphodiesterase activity *in vitro*, but absent from proteins that lack *in vitro* PDE activity. FimX lacks a number of the residues which appear to characterize active PDEs, though they are present in the majority of *P. aeruginosa* EAL domain containing proteins. Of note, a very recent publication from Kulesekara *et al.* (2006) reported that no PDE activity above background could be detected in a whole-cell lysate of PA14 in which FimX was expressed from the low-copy number plasmid pMMB67 under control of the *tac* promoter. Indeed, only five of the 21 *P. aeruginosa* EAL domain-containing proteins expressed and assayed in this fashion by these authors showed detectable PDE activity, and none of the five possessed both GGDEF and EAL domains. In our hands, purified His_6-FimX is less active than our positive control, CC3396, but nonetheless reproducibly demonstrates PDE activity in the presence of GTP. Like most GGDEF and EAL domain proteins, FimX contains additional domains that are likely to modulate its activity *in vivo* and perhaps *in vitro*. We are currently testing the hypotheses that activating signals mediated by the REC and/or PAS domains of the protein modulate its PDE activity.

FimX localizes to the pole in a manner dependent on N-terminal sequences and enzymatic activity

The DGC activity of *C. crescentus* PleD is increased by phosphorylation of Asp 53, which lies within the N-terminal response regulator domain of this protein (Paul *et al.*, 2004). Phosphorylation is also critical for targeting PleD to the emerging stalked pole; however, DGC activity is not important for subcellular localization, as a PleD allele carrying an inactivating point mutation in the GGEEF motif ($PleD_{GG368DE}$) is still correctly targeted to the stalked pole (Paul *et al.*, 2004). Thus PleD illustrates two further features of GGDEF/EAL domain proteins. Many contain additional signal transduction domains, which can control DGC or PDE activity temporally, in response to specific cues, and many show subcellular localization, which may serve to restrict production and/or degradation of c-di-GMP spatially. FimX possesses two such amino terminal domains, namely REC (response regulator) and PAS domains. No candidate phosphoacceptor aspartate can be identified in the REC domain. Deletion of the REC domain resulted in a FimX allele which was no longer localized to the bacterial pole. This is most likely because the ΔREC deletion also removes amino acids which may serve as a polar localization signal for FimX (Huang *et al.*, 2003), although our experiments do not rule out an independent signalling function for this domain.

RFP–FimX predominantly localizes to a single pole; however, both RFP–FimX(GDSIF→AASIF) and RFP–FimX(EVL→AAA) show predominantly bipolar localization in a Δ*fimX* background. As these two point mutant alleles do not support twitching motility, we also expressed the RFP fusions in wild-type PA103. RFP–FimX(GDSIF→AASIF) and RFP–FimX(EVL→AAA) remained predominantly bipolar, however, despite being expressed in a background where twitching motility occurred. Thus, residues within the ΔREC domain are required to bring FimX to the poles, and enzymatic

activity further restricts FimX to a single pole. We do not know if RFP–FimX resides at the piliated or non-piliated pole.

FimX is required for in vitro cytotoxicity, but not for in vivo virulence

Although Δ*fimX* bacteria are severely attenuated for cyto-toxicity towards tissue culture cells, the Δ*fimX* strain is slightly more virulent than PA103 in the murine acute pneumonia model. A similar discordance has been observed for other *P. aeruginosa* mutants that fail to assemble functional pili and are no longer cytotoxic towards tissue culture cells, but still demonstrate virulence *in vivo* (Comolli *et al.*, 1999b; Kulesekara *et al.*, 2006). It is not clear why tfp appear dispensable in murine models of acute infection: possibly the absence of tfp diminishes the ability of the innate immune system to recognize and clear *P. aeruginosa*, as suggested by observations that pili are required for non-opsonic phagocytosis of *P. aeruginosa* by macrophages and neutrophils (Speert *et al.*, 1986; Kelly *et al.*, 1989).

A common theme emerging from studies of GGDEF and EAL domain proteins is that they often regulate multicellular bacterial behaviour, in large part by altering extracellular matrix components synthesized by bacteria (Romling *et al.*, 2005). Thus, the assembly of other types of adhesive organelles, such as the *P. aeruginosa* cup fimbriae, appears to be linked to GGDEF/EAL domain proteins (Vallet *et al.*, 2001; D'Argenio *et al.*, 2002), as does the production of exopolysaccharides in a variety of bacterial species (Tal *et al.*, 1998; Ausmees *et al.*, 1999; Zogay *et al.*, 2001; Spiers *et al.*, 2002). Such multicellular behaviours are likely to be very significant for *P. aeruginosa* colonization and infection of cystic fibrosis patients, in whom bacteria grow as biofilms (Singh *et al.*, 2000). Indeed, *P. aeruginosa* biofilm formation can be strongly influenced by overexpression of exogenous DGC and PDE proteins (Simm *et al.*, 2004); thus, it is to be expected that some of the many endogenous GGDEF and EAL domain proteins within this organism will also influence biofilm formation. Strain PA103 does not form robust biofilms (T.S. Murray and B.I. Kazmierczak, unpubl. results); thus, evaluating the role of FimX in biofilm formation and in models of chronic lung infection will require introducing the Δ*fimX* mutation into other strains, as we are doing.

Experimental procedures

Sequence analysis

Sequences of EAL domain-containing proteins were downloaded from the Pseudomonas Genome Project (http://www.pseudomonas.com) (Stover *et al.*, 2000). Multiple sequence alignment was carried out using CLUSTALW (Chenna *et al.*, 2003), available at website http://www.ebi.ac.uk/clustalw/index.html. The alignment was subsequently manually adjusted. The *Gluconacetobacter xylinum* PdeA1 EAL domain sequence was included in the alignment to allow comparison with the results of Schmidt *et al.* (2005).

Bacterial strains and media

Bacterial strains were routinely cultured in LB or VBM medium with antibiotics as required at the following concentrations: ampicillin, 100 μg ml^{-1} for *E. coli*; carbenicillin, 200 μg ml^{-1} for *P. aeruginosa*; gentamicin, 10 μg ml^{-1} for *E. coli* or 100 μg ml^{-1} for *P. aeruginosa*; tetracycline, 20 μg ml^{-1} for *E. coli* or 100 μg ml^{-1} for *P. aeruginosa*. All strains were maintained at −80°C as 15% glycerol stocks. Bacteria were grown in MinS media containing 10 mM NTA (Nicas and Iglewski, 1984) to evaluate secretion via the TTSS as previously described (Laskowski *et al.*, 2004). All antibiotics were purchased from Sigma or USB. Bovine serum albumin (BSA), Fraction V was purchased from USB. A list of bacterial strains and plasmids used in this study is shown in Table 2.

Strain construction

All PCR primers employed in this study were ordered from Invitrogen, unless otherwise specified. They are listed in Table 3, and are based on the PA01 genome sequence (http://ww.pseudomonas.com) (Stover *et al.*, 2000). All amplifications were carried out with Pfu Turbo polymerase (Invitrogen), using PA103 genomic DNA as template, unless otherwise specified. PCR products were subcloned into pGEM-T Easy (Promega) and sequenced to confirm that no mutations were introduced during amplification. All intermediate cloning steps were performed using XL1-Blue *E. coli* (Stratagene). Plasmids were introduced into *E. coli* strains by electroporation (Sambrook *et al.*, 1989) and transformed into chemically competent *P. aeruginosa* (Mattick *et al.*, 1987) unless otherwise specified.

An unmarked, in-frame deletion of aa 15–685 of FimX in PA103 (Δ*fimX*) was constructed by allelic exchange (Schweizer and Hoang, 1995). Briefly, N-terminal (500 bp) and C-terminal (790 bp) regions flanking *fimX* were amplified using the primer pairs *fimX*-N1/*fimX*-N2 and *fimX*-C1/*fimX*-C2 respectively. The amplified regions were subcloned in tandem into the gene replacement vector pEX100T to generate pKO–FimX. This construct was transformed into *E. coli* S17-1 and mobilized into PA103 by mating. Carbenecillin-resistant exconjugants (merodiploids) were then resolved by growth on VBM plus 5% sucrose as described previously (Garrity-Ryan *et al.*, 2000). Potential mutants were screened by PCR and confirmed by Southern blot (data not shown). An identical strategy was used to construct ΔUTΔ*fimX*.

Cloning of FimX

A 2.9 kb BamHI-MfeI fragment containing the FimX open reading frame (ORF) plus 400 bp upstream and 421 bp downstream was subcloned from cosmid pMO012502 into the BamHI–EcoRI sites of pUCP-SK to generate pFimX (pMLD9). To facilitate subsequent cloning steps, several restriction sites within the multiple cloning site of pMLD9 were removed by digesting the plasmid with EcoRV and KpnI, blunting the KpnI site, and religating the plasmid. We confirmed that the EcoRV, KpnI and intervening HindIII, ClaI and XhoI sites were no longer present in this vector, which we named pMLD9x.

BB2 epitope-tagged constructs

A BB2 epitope tag (EVHTNQDPLD) was inserted immediately after the initiating methionine of FimX; codon usage was chosen to reflect codon bias within FimX and to create an ApaLI site within the tag sequence. The epitope tag sequence was incorporated into PCR primers BB2-B and BB2-C. Using pMLD9 as a template, the promoter region and amino-terminal portion of FimX (from the BamHI site to an internal XhoI site) were amplified with primer pairs BB2-A/BB2-B and BB2-C/BB2-D. The resulting PCR products were gel-purified, digested with ApaLI and ligated. Products of the ligation reaction were analysed by agarose gel electrophoresis, and the fragment corresponding to the ligation product of BB2-AB plus BB2-CD was cloned into pGEM-T Easy. We confirmed the in-frame incorporation of the BB2 epitope tag and the absence of any other mutations by sequencing. This fragment was then used to replace the BamHI-XhoI fragment of pMLD9x to create pBB2–FimX.

Domain deletion constructs

A deletion (aa 67–147, inclusive) removing the majority of the REC domain was constructed by PCR amplifying a *c.* 330 bp fragment of FimX which encompasses sequences encoding aa 148–242. The 5′ primer added a XhoI site to the PCR product, while the 3′ end of the PCR product contains a BsiW1 site present in the *fimX* sequence. This PCR product was subcloned into pGEM-T Easy (Promega), confirmed by sequencing, then

used to replace the *c*. 500 bp XhoI-BsiW1 region within pMLD9x (which contains aa 65–241 of FimX), resulting in pFimXΔREC. pBB2–FimXΔREC was constructed by replacing the XhoI-BsiW1 region of pBB2–FimX with the same PCR product.

The GGDEF domain was deleted as follows. Primers GGDEF-1 and GGDEF-2 were used to amplify a region corresponding to aa 65–252 of FimX; likewise, primers GGDEF-5 and GGDEF-4 amplified the region corresponding to aa 444–618 of FimX. KpnI sites were engineered into primers GGDEF-2 and GGDEF-3. The products of the two PCR reactions, GGDEF 1–2 and GGDEF 5–4, were gel-purified, digested with KpnI and ligated. Products of the ligation reaction were analysed by agarose gel electrophoresis, and the fragment corresponding to the ligation product of GGDEF 1–2 plus GGDEF 5–4 was cloned into pGEM-T Easy. Sequencing confirmed the in-frame deletion of aa 253–443 (inclusive) and the addition of two new amino acids (valine-proline) corresponding to the new KpnI site. This fragment was then used to replace the XhoI-ClaI fragment (encompassing aa 65–618 of FimX) of pMLD9x and pBB2–FimX, resulting in plasmids pFimXΔGGDEF and pBB2–FimXΔGGDEF respectively.

The EAL domain of the protein was deleted by linker mutagenesis. Briefly, pMLD9x and pBB2–FimX were digested with NruI, which cuts these plasmids once at a position corresponding to aa 444 of FimX. An excess of the EAL oligo was then ligated into this blunt site. The EAL oligo inserts three tandem stop codons in frame after aa 444 of FimX, effectively removing the carboxy-terminal EAL domain. A novel KpnI site is also introduced by this mutagenic oligo, which facilitated screening of products of the mutagenesis. The resulting plasmids were named pFimXΔEAL and pBB2–FimXΔEAL.

RFP fusion protein constructs

The RFP control plasmid, pRFP, was constructed by subcloning a SacI–HindIII fragment from tdimer2 into the SacI–HindIII sites of pUCP-SK. This allows the RFP dimer to be constitutively expressed from the *lac* promoter of pUCP-SK. RFPdimer sequences were introduced as amino-terminal in-frame fusions into pFimX as follows. PCR primers RFP-F and RFP-R were used to amplify RFPdimer from tdimer2; the PCR product was cloned into pGEM-T Easy. A BspHI fragment containing RFPdimer sequences was subcloned into the NcoI site of pFimX. Correct orientation of the insert was confirmed by checking the BamHI/NcoI restriction pattern. The same strategy was used to introduce N-terminal RFP-dimer sequences into pFimXΔREC, pFimX(GDSIF→AASIF) and pFimX(EVL→AAA).

Single-copy complementation

Wild-type FimX, BB2–FimX and each of the domain deletion constructs were cloned into the vector pCTX-2, which was then used to recombine these alleles into the *attB* site as previously described (Laskowski *et al*., 2004). Specific details of the subcloning strategy used for each construct are available upon request. Flp recombinase was subsequently introduced into each strain, allowing vector backbone sequences to be removed by virtue of flanking FRT sites (Hoang *et al*., 1998). Each allele was expressed under control of the native *fimX* promoter, which was contained within the fragments cloned into pCTX-2. Insertion of each sequence into the *attB* site was confirmed by PCR amplification using Ser-up and Ser-down primers, followed by diagnostic restriction digests of the resulting PCR products (data not shown).

Construction of point mutants

The EcoR1–HindIII fragment of pFimX, which contains the GGDEF and EAL domains of FimX, was subcloned into pBluescript-KS to create a template for site-directed mutagenesis. Mutagenic oligos GDSIF/AASIF forward and reverse and EVL/AAA forward and reverse

(listed in Table 2) were ordered from the DNA Synthesis Facility (Department of Pathology, Yale University) and gel-purified prior to use. PCR was carried out using Pfu Turbo (Invitrogen); annealing and extension conditions are available upon request. PCR products were treated with DpnI, which digests methylated and hemi-methylated DNA prior to transformation into XL1-Blue; this step selectively degrades template DNA. Introduction of the desired mutations was confirmed by sequencing of the entire EcoR1–HindIII insert. We also confirmed that no unwanted mutations were introduced during this process. The mutations were transferred into our series of expression vectors by subcloning; specific details of the strategy used to construct particular vectors are available upon request.

Construction, expression and purification of His_6 fusion proteins

Wild-type FimX, FimX(GDSIF→AASIF) and FimX(EVL→AAA) were subcloned in-frame with an amino-terminal 6× His tag in the pBAD/His B vector (Invitrogen); specific details of the subcloning strategy used for each construct are available upon request. The region of the construct spanning the joint between the His_6 tag and the FimX ORF was sequenced to confirm that each coding sequence was in frame with the epitope tag. pBAD-His_6FimX, pBAD-His_6FimX(GDSIF→AASIF) and pBAD-His_6FimX(EVL→AAA) were transformed into *E. coli* Top10 (Invitrogen). Overnight cultures of plasmid carrying strains were diluted 1:100 into LB plus ampicillin and grown at 37°C with vigorous aeration to OD_{600}~0.8, at which point fusion protein expression was induced for 90 min by the addition of 0.2% arabinose. Bacteria were harvested by centrifugation (7000 *g* for 20 min), resuspended in 50 mM sodium phosphate pH 7.0/300 mM NaCl/5 mM β-mercaptoethanol/ 0.2 mg ml^{-1} PMSF and lysed by passage through a French pressure cell twice (14 000 psi). The lysate was cleared by centrifugation (20 000 *g* for 30 min) before incubation with Talon™ Metal Affinity Resin (BD Biosciences) at 4°C overnight. Protein was eluted with 150 mM imidazole and fractions assayed by SDS-PAGE. Fractions containing > 95% pure protein were pooled and dialysed against 25 mM Tris-HCl, pH 8.0/250 mM NaCl/5 mM β-mercaptoethanol for 12 h at 4°C. Protein concentrations were determined by BCA assay (Pierce).

Vectors expressing His_6 fusions of PleD*, PleD and CC3396 were generously provided by Ralf Paul and Urs Jenal (University of Basel) (Paul *et al.*, 2004; Christen *et al.*, 2005). PleD*-H6, PleD-H6 and CC3396-H6 were expressed and purified from *E. coli* BL21(DE3) pLysS as described above, except that protein expression was induced at OD_{600}~0.6 for 45 min by the addition of 0.5 mM IPTG.

Diguanylate cyclase assays

Methods described by Urs Jenal and colleagues were adapted as follows (Paul *et al.*, 2004; Christen *et al.*, 2005). Briefly, 1 μl of α-labelled [^{32}P]-GTP (3.33 pmol, 3000 Ci $mmol^{-1}$, Amersham) was added to 9 μl of reaction buffer containing 25 mM Tris-HCl, pH 8.0, 250 mM NaCl, 5 mM β-mercaptoethanol, 10 mM $MgCl_2$, $MnCl_2$ or $CaCl_2$ (as indicated) and 15 μM His_6-fusion protein (as indicated). Reactions were incubated at 25°C for 10–60 min and stopped by the addition of 2 μl of 0.5 M EDTA. Products were separated by TLC on PEI-cellulose plates (Macherey-Nagel), using 1:1.5 v/v saturated NH_4SO_4 and 1.5 M KH_2PO_4, pH 3.6 as the solvent. Products were visualized by exposing TLC plates to film (30 min to 12 h). Autoradiographs were scanned at 300 dpi and assembled into figures using Photoshop 7.0 (Adobe). The product of the PleD*-H6 reaction served as a control for the migration of c-di-GMP in this TLC system.

Synthesis of [^{32}P]-c-di-GMP

[^{32}P]-c-di-GMP was produced enzymatically by incubating 5 μl of α-labelled [^{32}P]-GTP (16.5 pmol, 3000 Ci $mmol^{-1}$, Amersham) in the presence of 50 μM PleD*-H6, 10 mM

$MgCl_2$, 25 mM Tris-HCl, pH 8.0, 250 mM NaCl and 5 mM β-mercaptoethanol for 45 min at 25°C. The protein was precipitated by heating at 95°C for 10 min followed by centrifugation at 20 000 *g* for 2 min. Conversion of GTP into c-di-GMP was confirmed by TLC on PEI-cellulose plates as described above. The clarified reaction was stored at −20°C; 1 μl was used as substrate per 10 μl PDE assay as described below.

Phosphodiesterase assays

A 10 μl reaction containing hexahistidine-tagged protein (15 μM), 10 mM $MgCl_2$, $MnCl_2$ or $CaCl_2$ (as indicated), 100 μM GTP (as indicated), 25 mM Tris-HCl, pH 8.0, 250 mM NaCl, 5 mM β-mercaptoethanol, and 1 μl of clarified c-di-GMP synthesis reaction (prepared as above) was incubated at 25°C for 10–60 min, then stopped by the addition of 2 μl of 0.5 M EDTA. Reaction products were separated by TLC on PEI-cellulose as described above and visualized by autoradiography. The product of CC3396-H6 incubation served as a positive control for the migration of pGpG in this TLC system. The spot identified as GMP co-migrated with cold GMP (Sigma) by TLC.

Western blotting

Bacterial cultures were grown overnight in LB with appropriate antibiotics. Bacteria were pelleted by centrifugation, then incubated for 10 min in 4% SDS at 100°C. Bacterial lysates were briefly sonicated (10–15 s) before being assayed for total protein concentration using the BCA assay (Pierce). Five to 25 μg of total protein per sample was loaded on 10% gels and separated by SDS-PAGE. Proteins were transferred to PVDF (Immobilon-P, Millipore) and blocked with 1× TBST plus 5% (w/v) dry milk for 30 min prior to incubation with primary antibody. Anti-BB2 hybridoma supernatant (1:100, kindly provided by C. Tschudi, Yale University) or polyclonal antiserum recognizing PA103 PilA (1:1000, kindly provided by J. Engel, UCSF) was diluted into TBST plus 5% (w/v) dry milk and incubated with membranes overnight at 4°C. Horseradish peroxidase-conjugated secondary antibodies (Bio-Rad) were used at a concentration of 1:2000. Membranes were incubated for 1 min in 100 mM Tris-HCl pH 8.5/225 μM coumaric acid (Sigma)/1.25 mM 3-aminophthalhydrazide (Fluka)/0.009% H_2O_2, and chemiluminescence was detected using an Image Station 2000R running 1D Image Analysis software v. 3.6 (Kodak).

Subsurface stab assay for twitching motility

Bacterial strains were picked from fresh plates and stabbed through LB agar to the agar/plastic interface using a sterile needle as previously described (Huang *et al.*, 2003). Plates were incubated overnight at 37°C, at which time a twitching zone was visible on the plastic surface. The diameter of the twitching zone was measured; for non-circular zones, the longest and shortest dimensions were measured and averaged.

Phage sensitivity

PO4 phage (kindly provided by Patricia Baynham, Thomas More College) was serially diluted and spotted onto soft agar containing wild-type PA103 or indicated isogenic mutants. Plaques were counted following overnight incubation at 37°C. Efficiency of plaque formation was calculated relative to PA103.

Pilin ELISA

Bacteria were grown overnight on LB plates (with supplements or antibiotics as indicated) at 37°C and harvested by scraping. The protocol of Comolli *et al.* (1999b) was followed with minor modification. Briefly, bacterial suspensions were adjusted in MEM-lite to OD_{600} = 1.0. Serial dilutions of the suspensions were prepared in MEM-lite and used to coat 96 well ELISA plates in triplicate for 2 h at 37°C. Antigen was fixed with methanol, then exposed to

polyclonal antiserum generated against PA103 PilA (1:500) (kindly provided by Joanne Engel, UCSF). ELISA plates were washed three times with ddH_2O prior to addition of alkaline phosphatase-conjugated anti-rabbit-IgG (1:1000–1:2000, Bio-Rad). Wells were developed using BluePhos Microwell phosphatase substrate system (KPL, Gaithersburg MD) according to manufacturer's instructions.

Transmission electron microscopy

Bacteria grown in LB broth plus appropriate antibiotics were gently diluted in ddH_2O, then allowed to bind to glow-discharged carbon grids for 1 min. Grids were stained for 2 min in 2% uranyl acetate, washed with ddH_2O twice (20 s), then briefly dried before imaging on a Tecnai 12 Biotwin microscope (Center for Cell and Molecular Imaging, Yale University).

Cytotoxicity assays

HeLa cells (ATCC) were cultured and passaged as described previously (Laskowski *et al.*, 2004). HeLa cells were plated in 24 well dishes at 5×10^4 cells $well^{-1}$ 48 h prior to infection. Bacteria were grown in LB as previously described and used at a moi of 10 for infections. Prior to infection, HeLa cells were washed with and placed in MEM-etc. Cells were centrifuged at 800 rpm for 3 min after adding bacteria. Lactate dehydrogenase (LDH) release was assayed at 2 hpi and 4 hpi with the LDH assay kit according to manufacturer's instructions (Takara).

Binding assays

HeLa cells were cultured and passaged as described above for cytotoxicity assays. Infections were carried out at a moi of 5–10 for 1 h; cells were centrifuged at 800 rpm for 3 min after adding bacteria. Infected cells were washed four times with PBS to remove non-adherent bacteria, then lysed with Hanks Buffered Salt Solution (HBSS) (Invitrogen) plus 0.25% Triton X-100 (USB). Bound plus internalized bacteria were enumerated by plating serial dilutions of the lysate to VBM plates.

Localization of RFP fusion proteins by immunofluorescence microscopy

Bacteria were picked from LB agar plates containing antibiotics as appropriate and gently resuspended in 20 μl of water. Two millilitres of bacterial suspension was spotted onto a microscope slide coated with 1% Gel-Gro (MP Biomedicals) prepared according to manufacturer's instructions. Bacteria were visualized using an Eclipse TMS 100 microscope and Plan Apo 60XA/1.40 oil immersion lens. Images were obtained with a RT monochrome CCD camera (Spot Diagnostic Instruments) and assembled with Photoshop 7.0 (Adobe).

Murine model of acute pneumonia

Eight- to 10-week-old female C57Bl/6 mice were obtained from NCI and housed under specific pathogen-free conditions. All studies were approved by the Yale University Institutional Animal Care and Use Committee. Infections were carried out as described previously (Laskowski *et al.*, 2004). Briefly, mice were lightly anaesthetized with methoxyflurane (2–4%), then infected intranasally with 40 μl of bacterial suspension, corresponding to *c.* 5×10^5 cfu of bacteria. The actual dose administered was determined by plating serial dilutions of the inoculum and counting cfu. Mice were euthanized at 16 hpi, and the liver and lungs were removed, homogenized and resuspended in HBSS plus 0.25% Triton X-100. The suspensions were passed through a sterile screen to obtain a uniform suspension and serial dilutions were plated on VBM to determine recovery.

Statistical analysis

Means and standard deviations were calculated using Excel spreadsheet software (Microsoft). *T*-tests, chi-square analyses and Mann–Whitney statistics were calculated using Prism 4.0 software (GraphPad).

Acknowledgments

This work was supported by start-up funds from Yale University School of Medicine (B.I.K.), and NIH Grants R01 AI054920 (B.I.K.) and T32 AI07210 (T.S.M.). We thank Patricia Baynham, Joanne Engel, Christine Jacobs-Wagner, Herbert Schweizer, Christian Tschudi, Ralf Paul and Urs Jenal for kindly providing phage stock, plasmids, strains and antibodies. We are especially grateful to Urs Jenal for helpful discussions regarding diguanylate cyclase and phosphodiesterase assays. We thank Alison Pardee (Pseudomonas Genetic Stock Center, East Carolina University School of Medicine) for providing cosmid pMO012502. We thank Marc Pypaert (Center for Cell and Molecular Imaging, Yale University) for advice and assistance with TEM.

References

Aldridge P, Jenal U. Cell cycle-dependent degradation of a flagellar motor component requires a novel-type response regulator. Mol Microbiol. 1999; 32:379–391. [PubMed: 10231493]

Ausmees N, Jonsson H, Hoglund S, Ljunggren HG, Lindberg M. Structural and putative regulatory genes involved in cellulose synthesis in *Rhizobium leguminosarum* bv. *trifolii*. Microbiology. 1999; 145:1253–1262. [PubMed: 10376842]

Bobrov AG, Kirillina O, Perry RD. The phosphodiesterase activity of the HmsP EAL domain is required for negative regulation of biofilm formation in *Yersinia pestis*. FEMS Microbiol Lett. 2005; 247:123–130. [PubMed: 15935569]

Bradley DE. A function of *Pseudomonas aeruginosa* PAO pili: twitching motility. Can J Microbiol. 1980; 26:146–154. [PubMed: 6105908]

Brookman JL, Stott AJ, Cheeseman PJ, Burns NR, Adams SE, Kingsman AJ, Gull K. An immunological analysis of Ty1 virus-like particle structure. Virology. 1995; 207:59–67. [PubMed: 7532885]

Chan C, Paul R, Samoray D, Amiot NC, Giese B, Jenal U, Schirmer T. Structural basis of activity and allosteric control of diguanylate cyclase. Proc Natl Acad Sci USA. 2004; 101:17084–17089. [PubMed: 15569936]

Chenna R, Sugawara H, Koike T, Lopez R, Gibson TJ, Higgins DG, Thompson JD. Multiple sequence alignment with the Clustal series of programs. Nucleic Acids Res. 2003; 31:3497–3500. [PubMed: 12824352]

Chi E, Mehl T, Nunn D, Lory S. Interaction of *Pseudomonas aeruginosa* with A549 pneumocyte cells. Infect Immun. 1991; 59:822–828. [PubMed: 1671777]

Christen M, Christen B, Folcher M, Schauerte A, Jenal U. Identification and characterization of a cyclic di-GMP specific phosphodiesterase and its allosteric control by GTP. J Biol Chem. 2005; 280:30829–30837. [PubMed: 15994307]

Comolli J, Waite L, Mostov K, Engel JN. The interaction of *Pseudomonas aeruginosa* pili and asialo-GM1 stimulates epithelial cell cytotoxicity and bacterial internalization. Infect Immun. 1999a; 67:3207–3214. [PubMed: 10377092]

Comolli J, Hauser A, Waite L, Whitchurch C, Mattick J, Engel J. PilU and PilT are required for cytotoxicity and virulence of *Pseudomonas aeruginosa*. Infect Immun. 1999b; 67:3625–3630. [PubMed: 10377148]

D'Argenio DA, Calfee MW, Rainey PB, Pesci EC. Autolysis and autoaggregation in *Pseudomonas aeruginosa* colony morphology mutants. J Bacteriol. 2002; 184:6481–6489. [PubMed: 12426335]

De Medicis E, Paquette J, Gauthier JJ, Shapcott D. Magnesium and manganese contact of halophilic bacteria. Appl Environ Microbiol. 1986; 52:567–573. [PubMed: 16347151]

Doig P, Todd T, Sastry PA, Lee KK, Hodges RS, Paranchych W, Irvin RT. Role of pili in adhesion of *Pseudomonas aeruginosa* to human respiratory epithelial cells. Infect Immun. 1988; 56:1641–1646. [PubMed: 2897336]

Finck-Barbancon V, Goranson J, Zhu L, Sawa T, Wiener-Kronish JP, Fleiszig SMJ, et al. ExoU expression by *Pseudomonas aeruginosa* correlates with acute cytotoxicity and epithelial injury. Mol Microbiol. 1997; 25:547–557. [PubMed: 9302017]

Francis SH, Turko IV, Grimes KA, Corbin JD. Histidine-607 and histidine-643 provide important interactions for metal support of catalysis in phosphodiesterase-5. Biochemistry. 2000; 39:9591–9596. [PubMed: 10924156]

Frank DW. The exoenzyme S regulon of *Pseudomonas aeruginosa*. Mol Microbiol. 1997; 4:621–629. [PubMed: 9427393]

Garrity-Ryan L, Kazmierczak B, Kowal R, Comolli J, Hauser A, Engel J. The arginine finger domain of ExoT is required for actin cytoskeleton disruption and inhibition of internalization of *Pseudomonas aeruginosa* by epithelial cells and macrophages. Infect Immun. 2000; 68:7100–7113. [PubMed: 11083836]

Goodman AL, Kulasekara BR, Rietsch A, Boyd D, Smith RS, Lory S. A signaling network reciprocally regulates genes associated with acute infection and chronic persistence in *Pseudomonas aeruginosa*. Develop Cell. 2004; 7:745–754.

Hauser AR, Kang PJ, Engel J. PepA, a novel secreted protein of *Pseudomonas aeruginosa*, is necessary for cytotoxicity and virulence. Mol Microbiol. 1998; 27:807–818. [PubMed: 9515706]

Hoang TT, Karkhoff-Schweizer RR, Kutchma AJ, Schweizer HP. A broad-host-range Flp-FRT recombination system for site-specific excision of chromosomally-located DNA sequences: application for isolation of unmarked *Pseudomonas aeruginosa* mutants. Gene. 1998; 212:77–86. [PubMed: 9661666]

Hoch, JA.; Silhavy, TJ., editors. Two-Component Signal Transduction. Washington, DC: American Society for Microbiology Press; 1995.

Huang B, Whitchurch CB, Croft L, Beatson SA, Mattick JS. A minimal tiling path cosmid library for functional analysis of the *Pseudomonas aeruginosa* PAO1 genome. Microb Comp Genomics. 2000; 5:189–203. [PubMed: 11471833]

Huang B, Whitchurch CB, Mattick JS. FimX, a multidomain protein connecting environmental signals to twitching motility in *Pseudomonas aeruginosa*. J Bacteriol. 2003; 185:7068–7076. [PubMed: 14645265]

Kang PJ, Hauser AR, Apodaca G, Fleiszig S, Wiener-Kronish J, Mostov K, Engel JN. Identification of *Pseudomonas aeruginosa* genes required for epithelial cell injury. Mol Microbiol. 1997; 24:1249–1262. [PubMed: 9218773]

Kelly NM, Kluftinger JL, Pasloske BL, Paranchych W, Hancock RE. *Pseudomonas aeruginosa* pili as ligands for nonsopsonic phagocytosis by fibronectin-stimulated macrophages. Infect Immun. 1989; 57:3841–3845. [PubMed: 2572562]

Kirillina O, Fetherston JD, Bobrov AG, Abney J, Perry RD. HmsP, a putative phosphodiesterase, and HmsT, a putative diguanylate cyclase, control Hms-dependent biofilm formation in *Yersinia pestis*. Mol Microbiol. 2004; 54:75–88. [PubMed: 15458406]

Klausen M, Aaes-Jorgensen A, Molin S, Tolker-Nielsen T. Involvement of bacterial migration in the development of complex multicellular structures in *Pseudomonas aeruginosa* biofilms. Mol Microbiol. 2003a; 50:61–68. [PubMed: 14507363]

Klausen M, Heydorn A, Ragas P, Lambertsen L, Aaes-Jorgensen A, Molin S, Tolker-Nielsen T. Biofilm formation by *Pseudomonas aeruginosa* wild type, flagella and type IV pili mutants. Mol Microbiol. 2003b; 48:1511–1524. [PubMed: 12791135]

Kulesekara H, Lee VT, Brencic A, Liberati N, Urbach J, Miyata S, et al. Analysis of *Pseudomonas aeruginosa* diguanylate cyclases and phosphodiesterases reveals a role for bis-(3′-5′)-cyclic-GMP in virulence. Proc Natl Acad Sci USA. 2006; 103:2839–2844. [PubMed: 16477007]

Laskowski MA, Osborn E, Kazmierczak BI. A novel sensor kinase-response regulator hybrid regulates Type III secretion and is required for virulence in *Pseudomonas aeruginosa*. Mol Microbiol. 2004; 54:1090–1103. [PubMed: 15522089]

Liu PV. The roles of various fractions of *Pseudomonas aeruginosa* in its pathogenesis: identity of the lethal toxins produced *in vitro* and *in vivo*. J Infect Dis. 1966; 116:481–489. [PubMed: 4959184]

Mattick JS. Type IV pili and twitching motility. Annu Rev Microbiol. 2002; 56:289–314. [PubMed: 12142488]

Mattick JS, Bills MM, Anderson BJ, Dalrymple B, Mott MR, Egerton JR. Morphogenetic expression of *Bacteroides nodosus* fimbriae in *Pseudomonas aeruginosa*. J Bacteriol. 1987; 169:33–41. [PubMed: 2878919]

Merz AJ, So M, Sheetz MP. Pilus retraction powers bacterial twitching motility. Nature. 2000; 407:98–102. [PubMed: 10993081]

Nicas TI, Iglewski BH. Isolation and characterization of transposon-induced mutants of *Pseudomonas aeruginosa* deficient in production of exoenzyme S. Infect Immun. 1984; 45:470–474. [PubMed: 6086529]

O'Toole GA, Kolter R. Flagellar and twitching motility are necessary for *Pseudomonas aeruginosa* bio-film development. Mol Microbiol. 1998; 30:295–304. [PubMed: 9791175]

Paul R, Weiser S, Amiot NC, Chan C, Schirmer T, Giese B, Jenal U. Cell cycle-dependent dynamic localization of a bacterial response regulator with a novel di-guanylate cyclase output domain. Genes Dev. 2004; 18:715–727. [PubMed: 15075296]

Romling U, Gomelsky M, Galperin MY. C-di-GMP: the dawning of a novel bacterial signalling system. Mol Microbiol. 2005; 57:629–639. [PubMed: 16045609]

Salyers, AA.; Whitt, DD., editors. Bacterial Pathogenesis: A Molecular Approach. Washington, DC: American Society for Microbiology Press; 2002.

Sambrook, J.; Fritsch, EF.; Maniatis, T. Molecular Cloning: A Laboratory Manual. Cold Spring Harbor, NY: Cold Spring Harbor Laboratory Press; 1989.

Sastry PA, Finlay BB, Pasloske BL, Parachych W, Pearlstone JR, Smillie LB. Comparative studies of the amino acid and nucleotide sequences of pilin derived from *Pseudomonas aeruginosa* PAK and PAO. J Bacteriol. 1985; 164:571–577. [PubMed: 2997119]

Sato H, Frank DW, Hillard CJ, Feix JB, Pankhaniya RR, Moriyama K, et al. The mechanism of action of the *Pseudomonas aeruginosa* encoded type III cytotoxin, ExoU. EMBO J. 2003; 22:2959–2969. [PubMed: 12805211]

Schmidt AJ, Ryjenkov DA, Gomelsky M. The ubiquitous protein domain EAL is a cyclic diguanylate-specific phosphodiesterase: enzymatically active and inactive EAL domains. J Bacteriol. 2005; 187:4774–4781. [PubMed: 15995192]

Schweizer HP, Hoang TT. An improved system for gene replacement and xylE fusion analysis in *Pseudomonas aeruginosa*. Gene. 1995; 158:15–22. [PubMed: 7789804]

Simm R, Morr M, Kader A, Nimtz M, Romling U. GGDEF and EAL domains inversely regulate cyclic di-GMP levels and transition from sessility to motility. Mol Microbiol. 2004; 53:1123–1134. [PubMed: 15306016]

Simon R, Priefer U, Puhler A. A broad host range mobilization system for in vivo genetic engineering: transposon mutagenesis in gram negative bacteria. Biotechnology. 1983; 1:784–791.

Singh PK, Schaefer AL, Parsek MR, Moninger TO, Welsh MJ, Greenberg EP. Quorum-sensing signals indicate that cystic fibrosis lungs are infected with bacterial biofilms. Nature. 2000; 407:762–764. [PubMed: 11048725]

Speert DP, Loh BA, Cabral DA, Salit IE. Nonopsonic phagocytosis of nonmucoid *Pseudomonas aeruginosa* by human neutrophils and monocyte-derived macrophages is correlated with bacterial piliation and hydrophobicity. Infect Immun. 1986; 53:207–212. [PubMed: 2873104]

Spiers AJ, Kahn SG, Bohannon J, Travisano M, Rainey PB. Adaptive divergence in experimental populations of *Pseudomonas fluorescens*. I. Genetic and phenotypic bases of wrinkly spreader fitness. Genetics. 2002; 161:33–46. [PubMed: 12019221]

Stover C, Pham X, Erwin A, Mizoguchi S, Warrener P, Hickey M, et al. Complete genome sequence of *Pseudomonas aeruginosa* PA01, an opportunistic pathogen. Nature. 2000; 406:959–964. [PubMed: 10984043]

Sundin C, Wolfgang M, Lory S, Forsberg A, Frithz-Lindsten E. Type IV pili are not specifically required for contact dependent translocation of exoenzymes by *Pseudomonas aeruginosa*. Microb Pathog. 2002; 33:265–277. [PubMed: 12495673]

Tal R, Wong HC, Calhoon R, Gelfand D, Fear AL, Volman G, et al. Three *cdg* operons control cellular turnover of cyclic di-GMP in *Acetobacter xylinum*: genetic organization and occurrence of conserved domains in isoenzymes. J Bacteriol. 1998; 180:4416–4425. [PubMed: 9721278]

Vallet I, Olson JW, Lory S, Lazdunski A, Filloux A. The chaperone/usher pathways of *Pseudomonas aeruginosa*: identification of fimbrial gene clusters (*cup*) and their involvement in biofilm formation. Proc Natl Acad Sci USA. 2001; 98:6911–6916. [PubMed: 11381121]

Watson AA, Alm RA, Mattick JS. Construction of improved vectors for protein production in *Pseudomonas aeruginosa*. Gene. 1996; 172:163–164. [PubMed: 8654979]

Whitchurch CB, Leech AJ, Young MD, Kennedy D, Sargent JL, Bertrand JJ, et al. Characterization of a complex chemosensory signal transduction system which controls twitching motility in *Pseudomonas aeruginosa*. Mol Microbiol. 2004; 52:873–893. [PubMed: 15101991]

Whitchurch CB, Beatson SA, Comolli JC, Jakobsen T, Sargent JL, Bertrand JJ, et al. *Pseudomonas aeruginosa fimL* regulates multiple virulence functions by intersecting with Vfr-modulated pathways. Mol Microbiol. 2005; 55:1357–1378. [PubMed: 15720546]

Woods DE, Straus DC, Johanson WG, Berry VK, Bass JA. Role of pili in adherence of *Pseudomonas aeruginosa* to mammalian buccal epithelial cells. Infect Immun. 1980; 29:1146–1151. [PubMed: 6107276]

Zhulin IB, Taylor BL. PAS domain S-boxes in archaea, bacteria and sensors for oxygen and redox. Trends Biochem Sci. 1997; 22:331–333. [PubMed: 9301332]

Zogay X, Nimtz M, Rohde M, Bokranz W, Romling U. The multicellular morphotypes of *Salmonella typhimurium* and *Escherichia coli* produce cellulose as the second component of the extracellular matrix. Mol Microbiol. 2001; 39:1452–1463. [PubMed: 11260463]

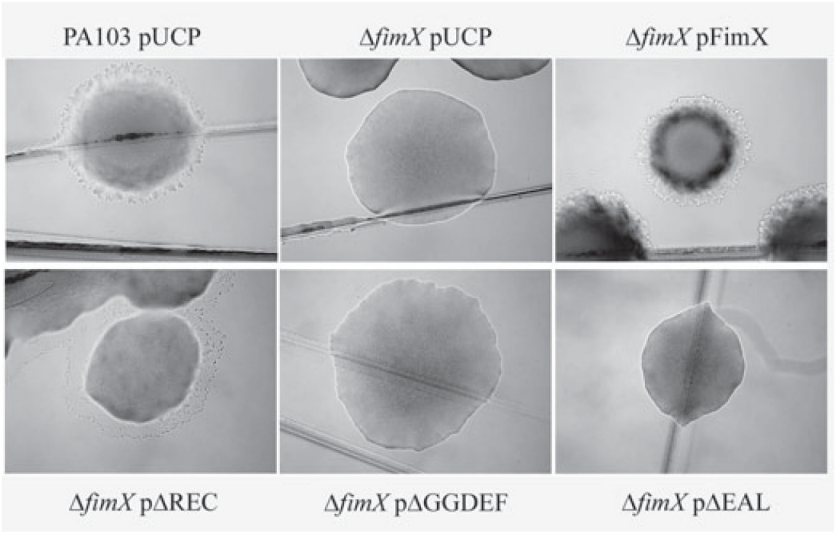

Fig. 1.

FimX is required for normal colony morphology and twitching motility. PA103 and Δ*fimX* strains were streaked to LB agar plates supplemented with carbenicillin (200 μg m^{-1}). Colonies were photographed under brightfield illumination at 40μ magnification after incubation at 37°C overnight followed by 24 h incubation at room temperature.

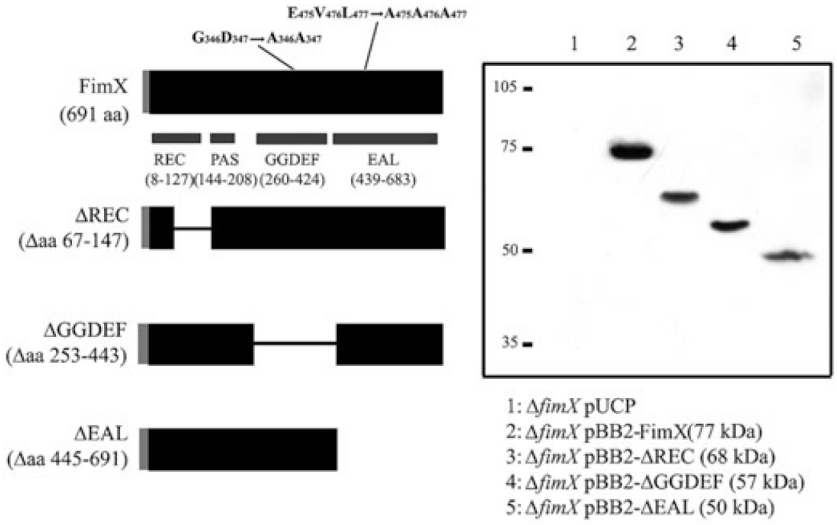

Fig. 2. Construction of FimX domain deletion mutants

A. Schematic showing domains of FimX. Amino acids deleted in each construct (inclusive) or mutated are indicated. The grey bar represents the amino-terminal BB2 epitope tag present in each construct.

B. Western blot of whole-cell lysates prepared from ΔfimX strains carrying indicated FimX constructs. Samples were normalized to total protein, separated by SDS-PAGE and transferred to PVDF membranes prior to incubation with anti-BB2 mAb. Calculated molecular weights for each construct are given in parentheses. Migration of molecular weight markers is indicated at left of gel.

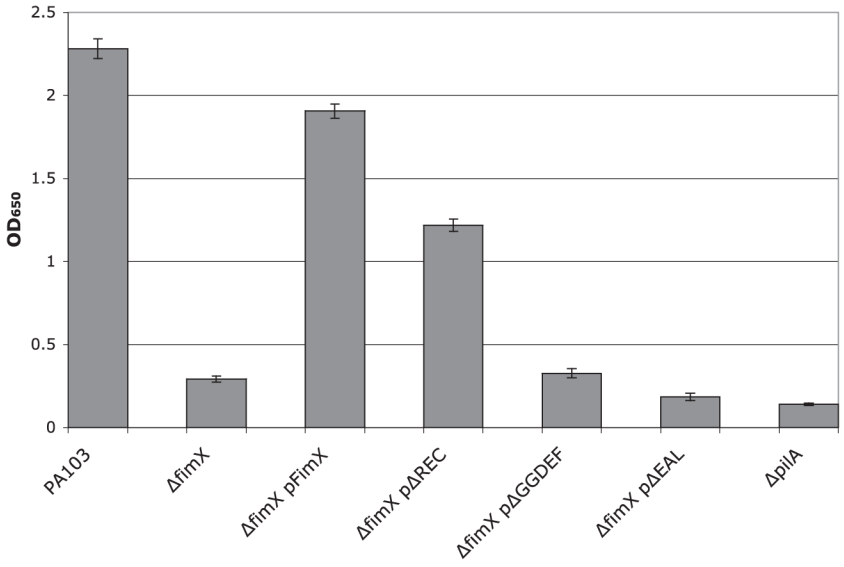

Fig. 3.

Total surface pili as determined by ELISA. Bacterial strains were harvested by scraping from LB agar plates after growth overnight at 37°C and resuspended in MEM-lite. Bacterial suspensions were normalized by OD_{600}, then serially diluted. Wells were coated in triplicate with diluted bacteria, fixed, and incubated with primary and secondary antibodies as described in *Experimental procedures*. Bars indicate mean ± SD of samples diluted to OD_{600} = 0.003 and are representative of four independent assays.

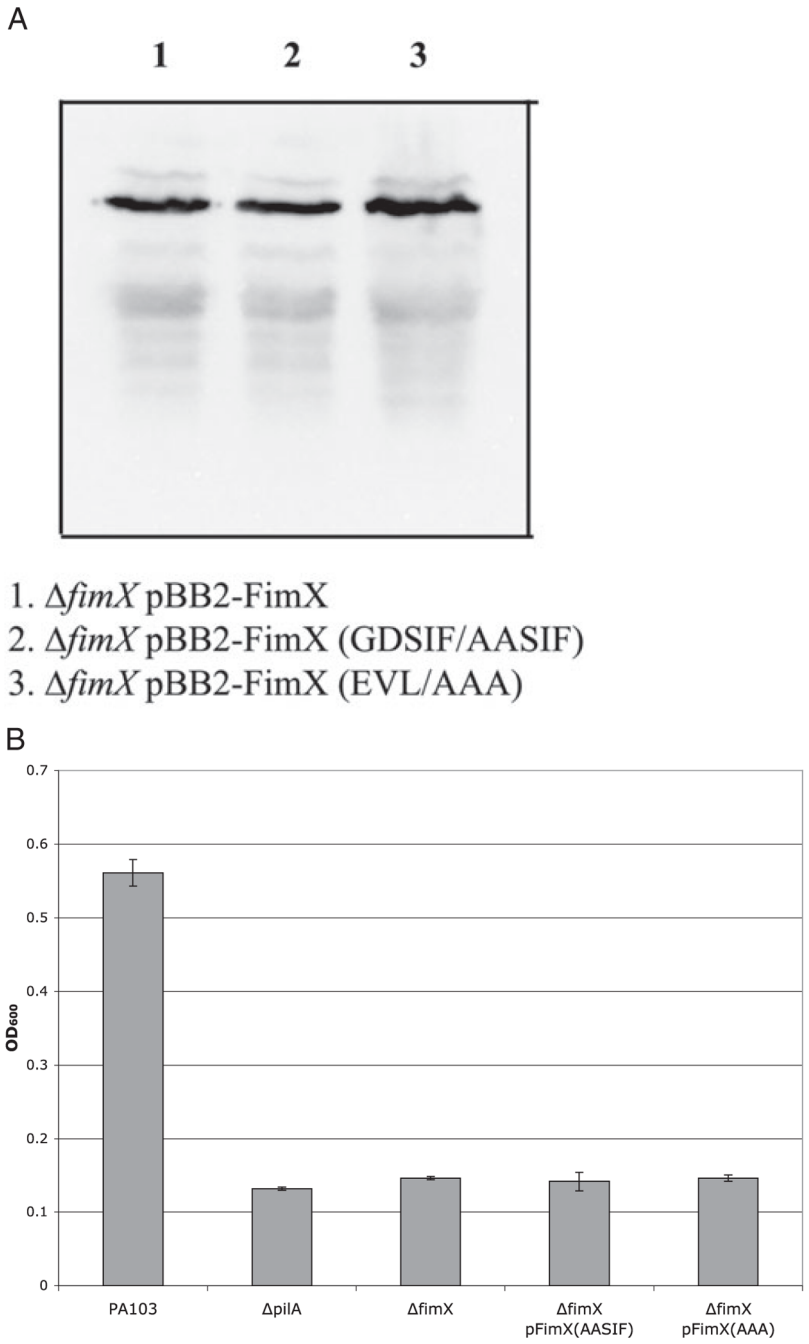

Fig. 4.

A. Expression of FimX point mutants. Whole-cell lysates were prepared from indicated bacterial strains. Samples were normalized to total protein prior to separation by SDS-PAGE, transferred to PVDF membrane and incubated with anti-BB2 mAb as detailed in *Experimental procedures*.

B. Expression of surface pili as measured by ELISA. Strains were harvested by scraping from agar plates, resuspended in MEM-lite, normalized to OD_{600}, and serially diluted. Wells were coated in triplicate, fixed, and incubated with primary and secondary antibodies as detailed in *Experimental procedures*. Bars indicate mean ± SD of samples diluted to OD_{600} = 0.003 and are representative of three independent assays.

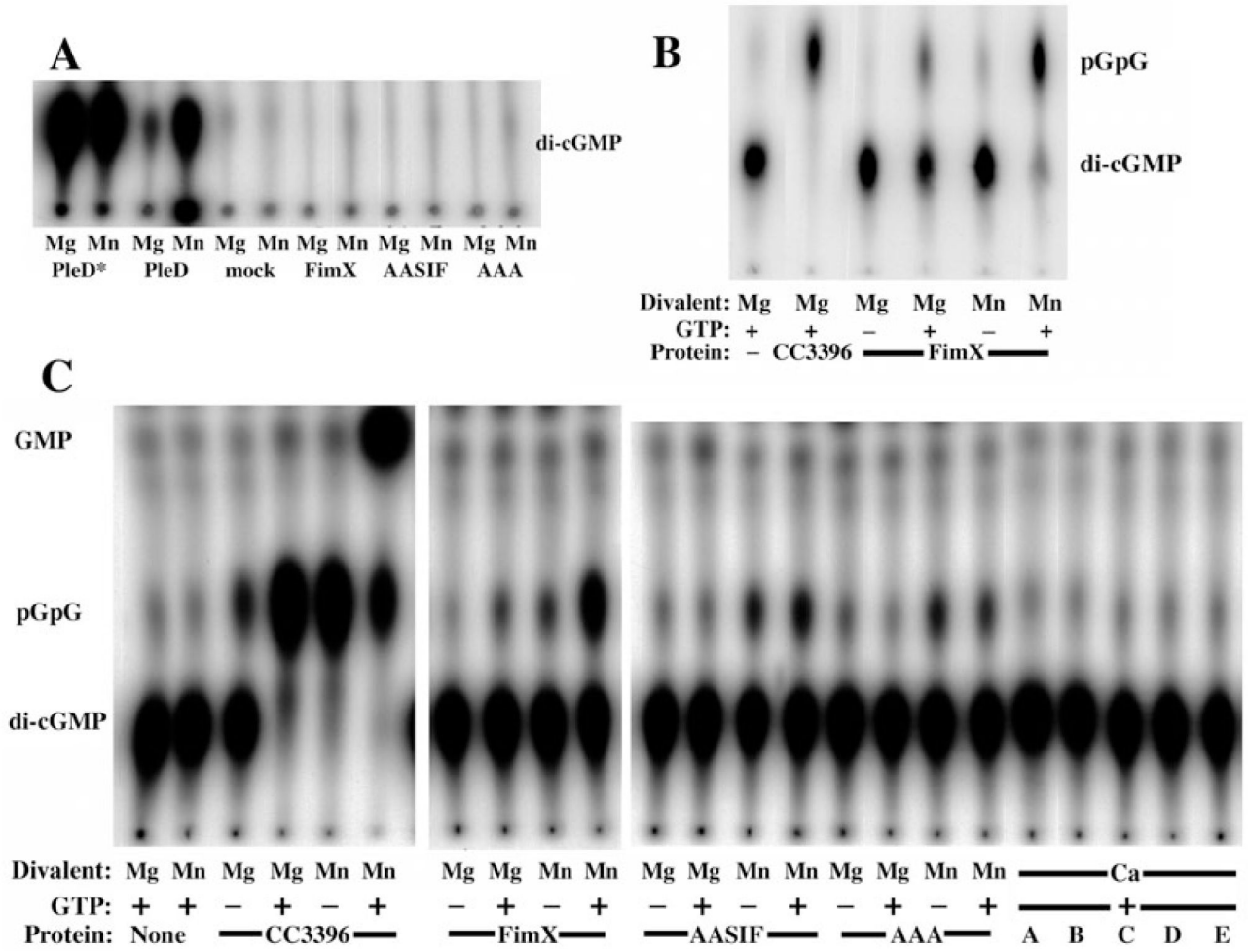

Fig. 5. FimX exhibits phosphodiesterase activity which is stimulated by GTP, but has no detectable DGC activity

A. TLC of DGC assay products. Purified hexahistidine-tagged proteins were assayed in the presence of 10 mM $MgCl_2$ or $MnCl_2$ (as indicated) for the ability to synthesize c-di-GMP from GTP. Reactions were stopped after 30 min by the addition of 0.5 M EDTA and assayed by TLC on PEI-cellulose as detailed in *Experimental procedures*.

B. TLC of phosphodiesterase assay products. Purified hexahistidine-tagged proteins were assayed in the presence of 10 mM $MgCl_2$ or $MnCl_2$ (as indicated), 100 μM GTP (as indicated) and [^{32}P]-c-di-GMP for 30 min. Reactions were stopped by the addition of 0.5 M EDTA and assayed by TLC on PEI-cellulose as detailed in *Experimental procedures*. No product with R_f(pGpG) was detected when substrate was incubated with $MgCl_2$ and GTP in the absence of protein.

C. Phosphodiesterase assay of wild-type FimX and point mutants. Hexahistidine-tagged proteins were incubated with [^{32}P]-c-di-GMP, 10 mM $MgCl_2$, $MnCl_2$, or $CaCl_2$ (as indicated) and 100 μM GTP (as indicated) for 60 min at 25°C. Reaction products were separated by TLC on PEI-cellulose as above. Lanes A–E correspond to: no protein (A); CC3396 (B); FimX (C); FimX(GDSIF→AASIF) (D); FimX(EVL→AAA) (E).

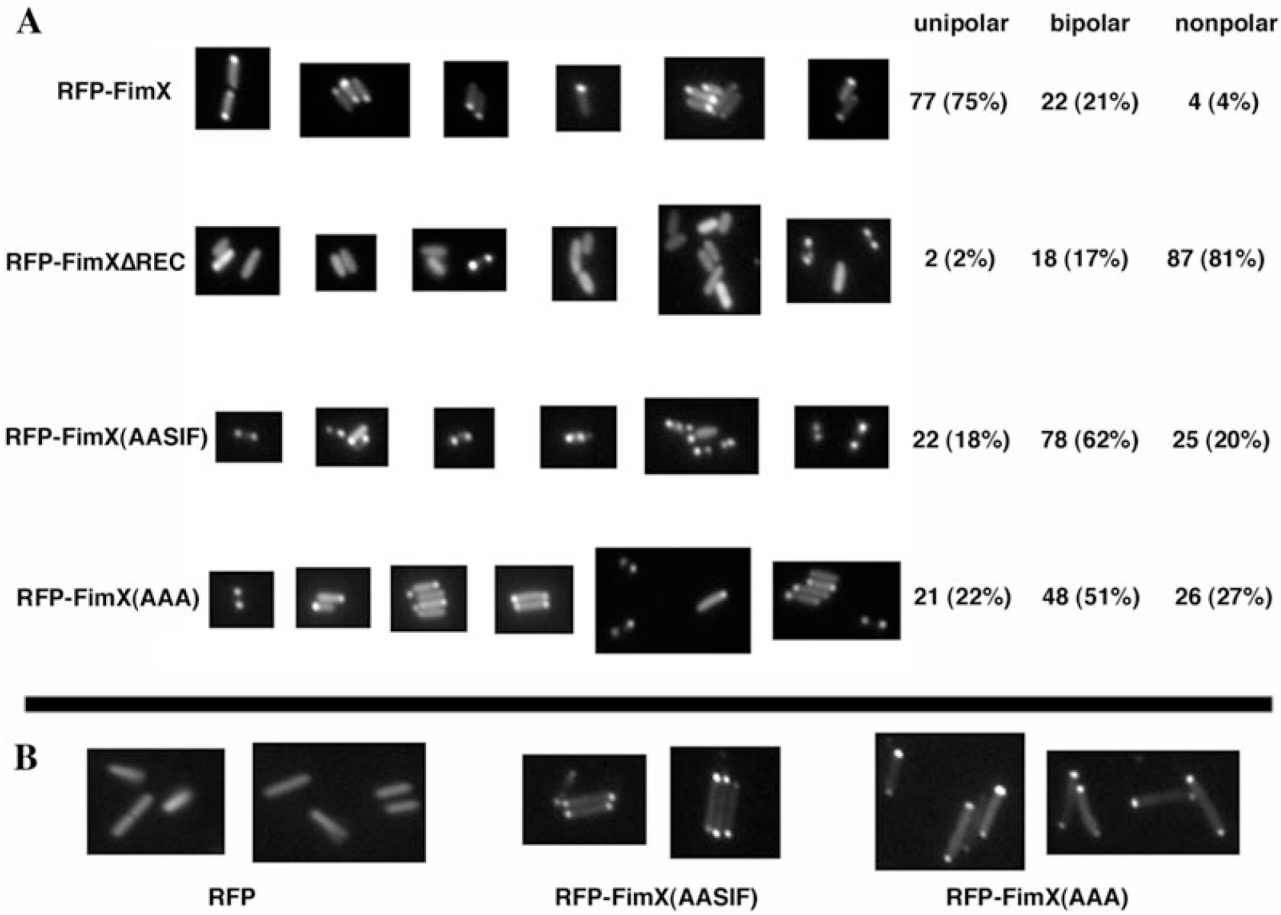

Fig. 6.

Localization of RFP–FimX fusion proteins by indirect immunofluorescence. Δ*fimX* (panel A) or PA103 (panel B) bacterial colonies expressing indicated RFP–FimX fusion constructs were picked from 2-day-old LB agar plates, resuspended in a drop of ddH_2O and spotted onto slides coated with a thin cushion of 1% Gel-Gro gellan. Bacteria were visualized and photographed as detailed in *Experimental procedures*.

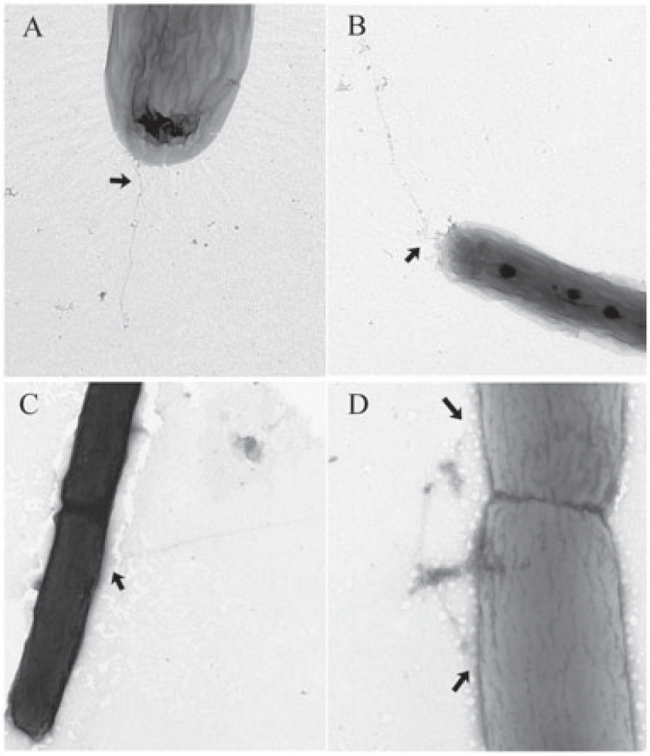

Fig. 7.

Visualization of tfp by electron microscopy. PA103 pUCP (panels A and B) and Δ*fimX* pFimXΔREC (panels C and D) bacteria were grown in LB supplemented with carbenicillin to OD_{600} = 0.6, then gently diluted 20- to 50-fold in ddH_2O prior to preparation and staining of grids, as detailed in *Experimental procedures*. Images were obtained with a Technai 12 Biotwin at magnifications between 13 000x and 30 000x. Negatives were scanned at 1200 dpi, then cropped, assembled and labelled using Photoshop 7.0. Arrows indicate locations at which pili emerge from the cell body.

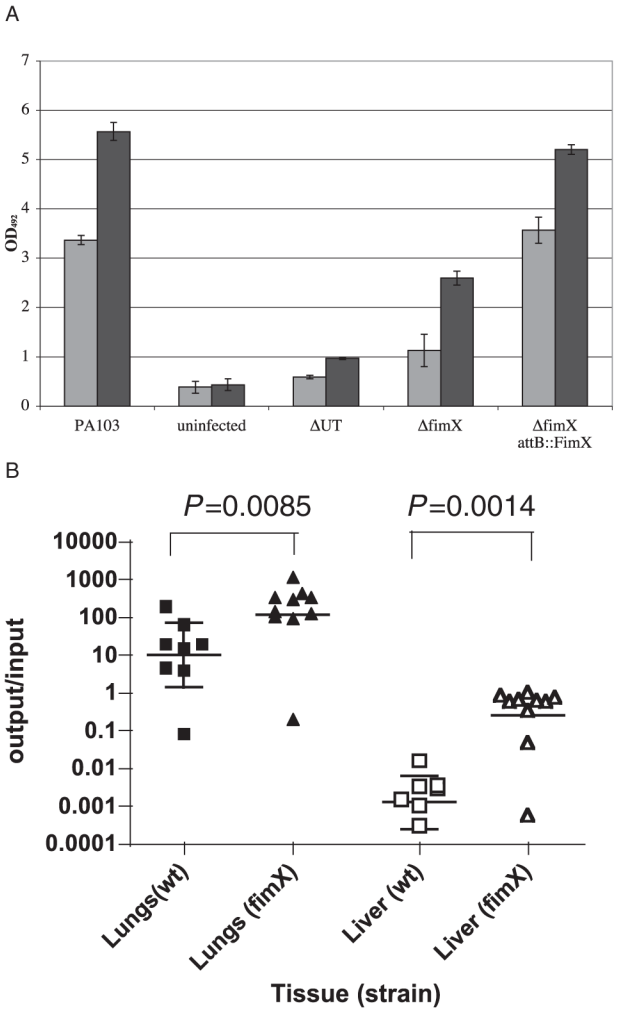

Fig. 8. FimX is required for cytotoxicity towards HeLa cells, but not for virulence in the murine model of acute pneumonia

A. LDH release measured from infected HeLa cells. Triplicate wells of HeLa cells were infected with indicated bacterial strains at a moi of 10. Culture supernatants were collected at 2 and 4 hpi and assayed for LDH activity. Bars indicate mean ± SD of a representative experiment.

B. Bacterial recovery from infected mice in an acute pneumonia model. Eight- to 10-week-old female C57Bl/6 mice were infected with *c.* 5×10^5 cfu of PA103 ($n = 8$) or Δ*fimX* ($n = 10$). Mice were euthanized at 16 hpi and the number of bacteria present in lungs and liver were determined as described in *Experimental procedures*. Results are expressed as the ratio of cfu recovered per g tissue (output) to cfu present in the inoculum (input); each animal is represented by a data point, while the bar shows the geometric mean for each group. The Mann–Whitney test was used to calculate *P*-values (two-tailed) for each pairwise comparison indicated.

Table 1

Tfp-dependent phenotypes of bacterial strains.

Strain	Efficiency of plaque formation[a]	Twitching zone (mm)[b]
PA103 pUCP	1.0	4.9 ± 0.4
Δ*pilA*	$< 1 \times 10^{-9}$	ND
Δ*fimX* pUCP	0.017 ± 0.008	0.7 ± 0.2
Δ*fimX* pFimX	1.13 ± 0.16	6.1 ± 0.2
Δ*fimX* pFimXΔREC	0.73 ± 0.15	3.3 ± 0.2
Δ*fimX* pFimXΔGGDEF	0.010 ± 0.003	3.0 ± 0.6
Δ*fimX* pFimXΔEAL	0.0072 ± 0.0051	1.8 ± 0.3
Δ*fimX* pFimX(GDSIF→AASIF)	0.043 ± 0.015	2.5 ± 0.4
Δ*fimX* pFimX(EVL→AAA)	0.012 ± 0.009	1.6 ± 0.3

[a] Efficiency of PO4 plaque formation expressed relative to strain PA103. Mean ± SD of three to six independent experiments.

[b] Twitching motility zone diameter, as measured by subsurface stab assay, performed with six replicates. Strains were assayed three to five times; mean ± SD of a typical experiment are shown.

Table 2

Bacterial strains and plasmids.

Bacterial strain or plasmid	Relevant characteristics	Source
E. coli XL1 blue	*recA1 endA1 gyrA96 thi-1 hsdR17 supE44 relA1 lac* [F′ *proAB lacI*^{q}*ZΔM15* Tn10(Tc^r)]	Stratagene
E. coli S17-1	Used for mating constructs into *P. aeruginosa; thi pro hsdR recA RP4-2* (Tc::Mu) (Km::Tn7)	Simon *et al.* (1983)
E. coli TOP10	F$^-$ *mcrA*Δ(*mrr-hsdRMS-mcrBC*) Φ 80*lacZ*ΔM15Δ *lacX74 recA1 araD139 galU galK*Δ(*ara-leu*)7697 *rpsL*(Str^r) *endA1 nupG*	Invitrogen
E. coli BL21 (DE3) pLysS	F$^-$ *dcm ompT hsdS*(rB$^-$mB$^-$) *gal* λ(DE3) [pLysS Cm^r]	Stratagene
PA103	Virulent lung isolate of *P. aeruginosa*, known type III-secreted effector proteins are ExoT and ExoU	Liu (1966)
Δ*fimX*	PA103 containing an in-frame deletion of aa 15–685 of *fimX* ORF	This study
Δ*fimX attB::*FimX	FimX under control of its own promoter integrated at *attB* site of Δ*fimX*	This study
Δ*fimX attB*::FimXΔREC	FimXΔREC under control of its own promoter integrated at *attB* site of Δ*fimX*	This study
Δ*fimX attB*::FimXΔGGDEF	FimXΔGGDEF under control of its own promoter integrated at *attB* site of Δ*fimX*	This study
Δ*fimX attB*::FimXΔEAL	FimXΔEAL under control of its own promoter integrated at *attB* site of Δ*fimX*	This study
ΔUT	PA103 containing in-frame deletions of *exoU* ORF (aa 330–571) and *exoT* ORF (aa 36–348)	Garrity-Ryan *et al.* (2000)
ΔUTΔ*fimX*	Δ*fimX* containing an in-frame deletion of aa 15–685 of *fimX* ORF	This study
Δ*pilA*	Gm^r cassette inserted into *pilA* in PA103; Gm^r	Whitchurch *et al.* (2005)
pGEM-T Easy	*E. coli* TA cloning vector; Ap^r	Promega
pBluescript-KS	*E. coli* cloning vector; Ap^r	Stratagene
tdimer2	RFP dimer cloned in pBluescript-KS	C. Jacobs-Wagner (Yale)
pMO012502	pLA2917 cosmid from PAO1 library containing PA4959 ORF; Tc^r	Huang *et al.* (2000)
pUCP-SK	*P. aeruginosa—E. coli* shuttle vector; Ap^r(Cb^r)	Watson *et al.* (1996)
mini-CTX-2	Contains *attP* site for integration at the *attB* site of the *P. aeruginosa* chromosome; Tc^r	Hoang *et al.* (1998)
pFLP2	Source of inducible Flp recombinase; Ap^r(Cb^r)	Hoang *et al.* (1998)
pEX100T	Allelic replacement suicide plasmid; Ap^r(Cb^r) *sacB oriT*	Schweizer and Hoang (1995)
pKO–FimX	N- and C-terminal regions flanking FimX ORF cloned in tandem in pEX100T; Ap^r(Cb^r)	This study
pFimX (pMLD9)	2.9 kb BamHI-MfeI fragment of pMO012502 cloned into pUCP-SK; Ap^r(Cb^r)	This study
pMLD9x	pFimX with altered MCS; Ap^r(Cb^r)	This study
pFimXΔREC	pFimX with sequences encoding aa 67–147 deleted; Ap^r(Cb^r)	This study
pFimXΔGGDEF	pFimX with sequences encoding aa 253–443 deleted; Ap^r(Cb^r)	This study
pFimXΔEAL	pFimX with stop codon inserted after aa 444; Ap^r(Cb^r)	This study
pFimX(GDSIF→AASIF)	pFimX with point mutations G346A D347A; Ap^r(Cb^r)	This study
pFimX(EVL→AAA)	pFimX with point mutations E475A V476A L477A; Ap^r(Cb^r)	This study
pBB2–FimX	pFimX with BB2 epitope tag inserted after initiating methionine of FimX; Ap^r(Cb^r)	This study
pBB2–FimXΔREC	pFimXΔREC with BB2 epitope tag inserted after initiating methionine of FimX; Ap^r(Cb^r)	This study

Bacterial strain or plasmid	Relevant characteristics	Source
pBB2–FimXΔGGDEF	pFimXΔGGDEF with BB2 epitope tag inserted after initiating methionine of FimX; $Ap^r(Cb^r)$	This study
pBB2–FimΔEAL	pFimXΔEAL with BB2 epitope tag inserted after initiating methionine of FimX; $Ap^r(Cb^r)$	This study
pBB2–FimX(GDSIF→AASIF)	pFimX(GDSIF→AASIF) with BB2 epitope tag inserted after initiating methionine of FimX; $Ap^r(Cb^r)$	This study
pBB2–FimX(EVL→AAA)	pFimX(EVL→AAA) with BB2 epitope tag inserted after initiating methionine of FimX; $Ap^r(Cb^r)$	This study
pRFP	SacI–HindIII fragment of tdimer2 subcloned into pUCP-SK(RFP under control of *lac* promoter); $Ap^r(Cb^r)$	This study
pRFP–FimX	pFimX with N-terminal RFP dimer fusion; $Ap^r(Cb^r)$	This study
pRFP–FimXΔREC	pFimXΔREC with N-terminal RFP dimer fusion; $Ap^r(Cb^r)$	This study
pRFP–FimX(GDSIF→AASIF)	pFimX(GDSIF→AASIF) with N-terminal RFP dimer fusion; $Ap^r(Cb^r)$	This study
pRFP–FimX(EVL→AAA)	pFimX(EVL→AAA) with N-terminal RFP dimer fusion; $Ap^r(Cb^r)$	This study
pBAD/His	Ap^r expression plasmid	Invitrogen
pET11	Ap^r expression plasmid	Stratagene
pET21	Ap^r expression plasmid	Stratagene
pHis6–FimX	pBAD/His; FimX, N-terminal His_6 tag	This study
pHis6–FimX(GDSIF→AASIF)	pBAD/His; FimX, N-terminal His_6 tag	This study
pHis6–FimX(EVL→AAA)	pBAD/His; FimX, N-terminal His_6 tag	This study
pCC2	pET11; *pleD*, C-terminal His_6 tag	Paul *et al.* (2004)
pRP89	pET11; *pleD**, C-terminal His_6 tag	Paul *et al.* (2004)
pMC24	pET21; CC3396, C-terminal His_6 tag	Christen *et al.* (2005)

Ap, ampicillin; Cb, carbenicillin; Gm, gentamicin; Km, kanamycin; Tc, tetracycline; Cm, chloramphenicol; Str, streptomycin.

Table 3

Primers and oligonucleotides used in this study.

RFP-F	**GCTCATGATGGCCTCCTCCGAGGAC**
RFP-R	GCTCATGAGGAACAGGTGGTGGCGG
fimX-N1	CTAGGATCCGATATCCGCCAGGTACGCAATGGC
fimX-N2	GATGAATTCCAGAATCAGCAGGCGG
fimX-C1	GATGAATTCTCCTCGGGAGACGAATG
fimX-C2	CGTGAAGCTTGATATCGCTTTCCAGCAGGACAG
BB2-A	CGCTGGATCCGCCAGGTACGCAATGG
BB2-B	TGGTGTGCACCTCCATGGAAAGGGCTCAGTCCGCG
BB2-C	GGAGGTGCACACCAACCAGGACCCGCTCGACGCCATCGAAAAGAAAACCATCCGC
BB2-D	CCGGGCTCGAGACACTCGCTGG
REC-3	GCTCACTCGAGTTGCTGCTCGAAGCTCGGTCGACGCCATCAC
REC-2	CGCCGTCGTACGTGGCGG
GGDEF-1	CTCAGCTCGAGCCCGGCGAG
GGDEF-2	GACTCGGTACCCCGCGGATCACCACCTGGATGC
GGDEF-4	CTCGGATCGATCTTGATGAACTGCA
GGDEF-5	GAGCGGTACCCATCGCGATCCTCCAGCAGG
EAL	CATAGTAATGAGGTACCTCATTACTATG
Ser-up	CGAGTGGTTTAAGGCAACGGTCTTGA
Ser-down	AGTTCGGCCTGGTGGAGCAACTCG
GDSIF/AASIF forward	GCCGACCTGGCGCGTTTCGCCGCTTCGATCTTCGCCGCC
GDSIF/AASIF reverse	GGCGGCGAAGATCGAAGCGGCGAAACGCGCCAGGTCGGC
EVL/AAA forward	CGGCGACAGCCACGAGAACTATGCAGCTGCTCTACGCCTCCTCAATCCGCAGGGCC
EVL/AAA reverse	GGCCCTGCGGATTGAGGAGGCGTAGAGCAGCTGCATAGTTCTCGTGGCTGTCGCCG

All primers are listed 5′ to 3′.